

# A New Method to Improve the Stability, Tensile Strength, and Heat Resistant Properties of Shape-Memory Epoxy Resins: Two-Stages Curing

He Sun,<sup>1</sup> Yuyan Liu,<sup>1</sup> Huifeng Tan,<sup>2</sup> Xingwen Du<sup>2</sup>

<sup>1</sup>School of Chemical Engineering and Technology, Harbin Institute of Technology, Harbin 150001, China

<sup>2</sup>School of Astronautics, Harbin Institute of Technology, Harbin 150001, China

Correspondence to: Y. Liu (E-mail: liuyy@hit.edu.cn)

**ABSTRACT:** In this article, we design a new thermal curing method: two-stage curing. The purpose of using this approach is to maintain the excellent shape-memory property of epoxy resin system after first stage curing, and the material can be folded in small size to storage or transportation and recover its original shape commodiously by heating temperature. Then, after second stage curing, the stability, glass transition temperature ( $T_g$ ), and tensile strength of material can be improved effectively. For this aim, a series of mixtures have been prepared. Differential scanning calorimetry (DSC), Fourier transform infrared spectroscopy (FTIR), tensile test, scanning electron microscope (SEM), dynamic mechanical analysis (DMA), and fold-deploy shape-memory test have been used to characterize the feasibility of two-stage curing process, curing degree, tensile strength, morphology, thermodynamic properties, and shape-memory performance of these polymers. DSC results show that two independent curing stages can be achieved successfully. Tensile tests and DMA results suggest that tensile strength and heat resistance have been improved after the second curing stage. SEM results reveal that the addition of latent curing agent do not change the fracture mechanism. Furthermore, the fold-deploy shape-memory tests prove that the composites after first stage curing possess excellent shape-memory property. © 2013 Wiley Periodicals, Inc. *J. Appl. Polym. Sci.* 2014, 131, 39882.

**KEYWORDS:** epoxy resins; shape-memory; two-stage curing

Received 9 June 2013; accepted 22 August 2013

DOI: 10.1002/app.39882

## INTRODUCTION

Shape-memory polymers (SMPs) represent an advanced class of stimuli-responsive materials, which can be deformed or fixed into a temporary shape and recover their original permanent shapes only upon appropriate external stimulus,<sup>1–4</sup> such as thermal treatment, light, electricity and vapor.<sup>5–8</sup> Although above various forms of external stimuli may be utilized as the recovery trigger, the thermally induced shape-memory effect is most typical where the recovery takes place with respect to a certain critical temperature. Here, thermoset shape-memory epoxy resins have attracted considerable attention because they hold a number of advantages, including lower cost, easy tunability in shape-memory characteristics, low density, high shape recoverability (up to 100%), and simple process ability.<sup>9–12</sup> However, there are two shortcomings for shape-memory materials. Firstly, SMPs have two-way shape memory reversibility, generally speaking, due to their permanent networks (net points) and reversible phase structures (switch segments).<sup>13–16</sup> It means that when the temperature is higher than the glass transition temperature ( $T_g$ ), the materials will either deform to a different

shape or restore to their original shapes. If the materials have been impacted by external force in high temperature, they would change their shapes. So the stability of the materials will be greatly affected by temperature. Second, SMPs have low crosslink density as a result of their inherent structures,<sup>17,18</sup> hence, mechanical strength and heat resistance are not very well. The objective of the present investigation is to overcome these two disadvantages by designing a new thermal curing method, two-stage curing process.

The two-stage curing method is different from conventional multistep curing or post-curing,<sup>19–21</sup> because it utilizes two different curing agents which trigger first-stage and second-stage curing independently (please note that two different hardeners rarely have reciprocity). The two-stage curing method can be plotted, as shown in Figure 1 and described as follows: (1) Two different curing agents, room temperature curing agent and latent curing agent, are added into the epoxy resin matrix synchronously. First-stage curing is triggered at room temperature, and the polymers form materials I with the desired spatial structure. During this curing period, the latent curing agent will

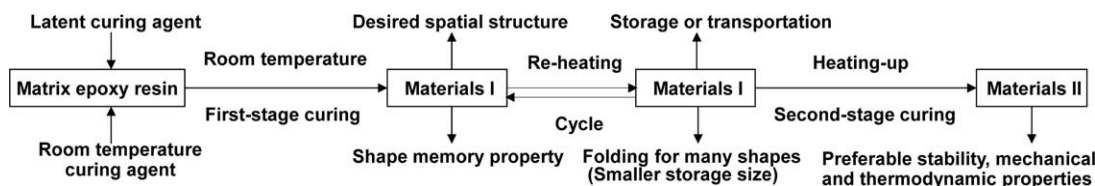


Figure 1. The two-stage curing method.

not be triggered by controlling the curing conditions. (2) If the spatial structure has big size, it is not convenient for storage or transportation, it can be folded into small size by heating temperature to making it becomes soft, such as tube, rectangle and so on. Materials I have the unique feature is that they possess shape memory effect (SME). Hence, the folded components can recovery to their original shapes by heating temperature to above  $T_g$ . In other words, the spatial structure can be fold-deploy for many times. It is useful and convenient for materials to test in different places. (3) Elevating heating temperature causes second stage curing if the components are used, and materials II are formed. After second-stage curing, the stability, heat resistance and mechanical strength of materials will be significantly improved. These kinds of materials can be utilized in fold-deploy structure, such supporting tube or space antenna, having a smaller store volume with preferable stability, mechanical and thermodynamic properties.

Here, the feasibility of two-stage curing technology, the control of curing conditions, shape memory property, stability, tensile strength, microstructure, and heat resistant of materials are examined respectively.

## EXPERIMENTAL

### Materials

The polymer matrix used in the current study was bisphenol A glycidyl ether epoxy resin E-51(WSE618), with epoxy value  $0.5 \pm 0.01$  (epoxy equivalent weight 196–204 g/eq). The epoxy resin possessed excellent shape-memory function, as shown in our previous researches.<sup>22,23</sup> The room temperature curing agent was a modified amine, 593; it was a transparent liquid and had long-chain structures, the amine value was 678.6 mg KOH/g, and the viscosity was 80–100 mPa·s (25°C). The latent curing

agent was  $\beta$ ,  $\beta'$ - dimethylamino ethoxy-1, 3, 6, 2-dioxin boron (594). All materials were used without further refinement. The chemical structures of reactants are shown in Figure 2.

### Preparation of Mixtures

For the first-stage curing, the theory mass of curing agent can be calculated from formula (1) due to 593 being an aliphatic amine:

$$Y = \left( \frac{M}{n-H} \right) \times K \quad (1)$$

where  $Y$  is the mass of curing agent used in 100 g epoxy resin,  $M$  is the molecular weight of amine,  $n_H$  is the number of active hydrogen in an amine molecular, here,  $n_H$  is 4, and  $K$  is the average epoxy value of E-51 (0.51).

For the second-stage curing, the theory mass of curing agent 594 is 12 wt % of the remaining uncured epoxy resin, the theory mass is obtained from FTIR test. Specific method is as follows: the theory mass of curing agent 594 in 9, 10, 11, 12, 13, and 14 wt % with the remaining uncured epoxy resin have been prepared. After curing, the products have been tested by FTIR technology. The FTIR results show that it can be still observed epoxy groups in  $908\text{--}930\text{ cm}^{-1}$  in the theory mass curing agent 594 in 9, 10, and 11 wt % systems, and not observed epoxy groups in 12, 13, and 14 wt % mixtures, indicating that the epoxy groups have been consumed completely when the theory mass of 594 exceeds 12 wt %.

Based on the above theoretical calculations, mixtures of 70, 80, 90, and 100% theory curing degree<sup>22</sup> were prepared. The theory curing degree was specific to first-stage curing, due, we suppose, to the fact that second stage curing was not triggered at the

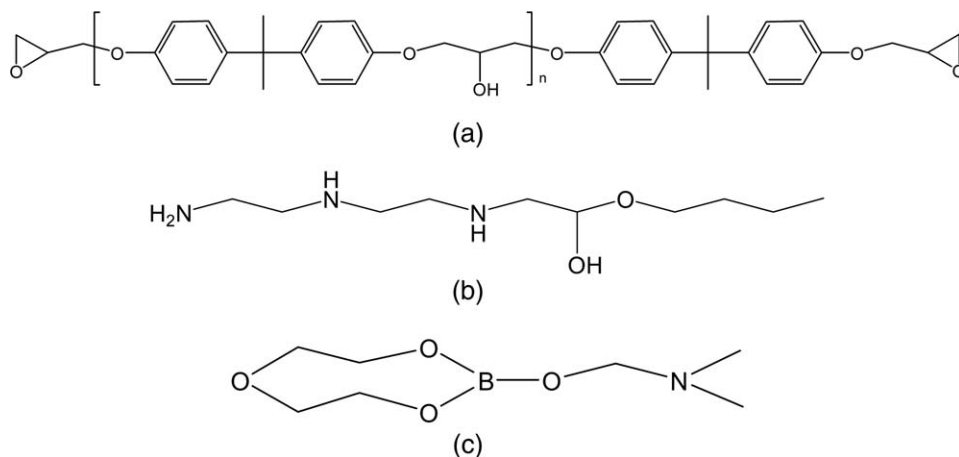


Figure 2. Chemical structures of epoxy resin and curing agents.

**Table I.** Serial Numbers of Different Mixtures

Theory curing degree (%)	70	80	90	100
E-51/593	EP70	EP80	EP90	EP100
E-51/593/594 <sup>a</sup> (Materials I)	EP70 I	EP80 I	EP90 I	-
E-51/593/594 <sup>b</sup> (Materials II)	EP70 II	EP80 II	EP90 II	-

<sup>a</sup>Second stage curing had not been triggered.

<sup>b</sup>Second stage curing had been triggered.

lower temperature. Serial numbers of different mixtures are listed in Table I.

For the various curing systems, two different curing schedules were used: (1) The mixtures of EP and EP I were cured at room temperature for 24 h, followed by curing in air oven at 80°C for 2 h, and then allowed to cool slowly to room temperature; (2) The mixtures of EP II were cured based on (1) first, then second-stage curing was performed at 130°C for 2 h, and curing at 170°C for 3 h, followed again by slow cooling to room temperature.

The cured EP and EP I systems were translucent; in addition, cured EP II mixtures were light yellow in color.

#### Characterization Methods

Non-isothermal DSC (Differential Scanning Calorimetry) measurements were performed with TA Instruments Q200 for data acquisition. DSC was calibrated with high purity indium, and experiments were conducted under a nitrogen flow of 20 cm<sup>3</sup>/min. In DSC experiments, all the samples were subjected to a dynamic DSC scan from 20 to 400°C/min at a heating rate of 10°C/min.

FTIR (Nicolet750 FTIR Spectrometer) was used to detect the epoxy absorption peaks in different mixtures. The specimens were prepared using the KBr pellet technique. The scanning scope was from 650 to 4000 cm<sup>-1</sup>.

Tensile testing was done using a tensile tester (Instron 5500R) to evaluate the mechanical properties of materials. Samples were dumbbell-shape, the width of effective part was 4 mm, and thickness was 2 mm. These specimens were elongated at the rate of 5 mm/min at room temperature.

The fracture surfaces of the notched impact samples were observed by scanning electron microscopy (SEM) using QUANTA 200FEI microscope. The fracture surfaces of specimens were coated with a gold layer prior to observation; the multiple of magnification was 1000.

Thermodynamic properties including the  $T_g$  and storage modulus of the composites were examined using a dynamic mechanical thermal analyzer (American, TA Q800) DMA, performed in a nitrogen atmosphere from 25 to 300°C under a three-point bending mode. The heating rate was set at 3°C/min, and the resonance frequency was adjusted to 1 Hz. The sample size was 25 mm × 5 mm × 1 mm.

To investigate the shape-memory performances of the composites, a bending fold-deploy shape-memory test was performed.

Bending deformation was widely employed for evaluating shape-memory properties of polymer materials due to a large deflection being easily obtained in the range of small strain through bending.<sup>24</sup> The test was done as follows<sup>22,23</sup>: first, a cured sample [size: 150 mm × (20 ± 1.5) mm × (2 ± 0.2) mm] was heated to its glass transition temperature ( $T_g$ ) (or  $T_g + 10^\circ\text{C}$ ,  $T_g + 20^\circ\text{C}$ ,  $T_g + 30^\circ\text{C}$ ) obtaining from DMA test, and then bent into a “U” shape encircling a central axis, with a radius of 6 mm; second, the U-shaped sample was cooled down to room temperature under a constant external force for several minutes, until the specimen became cool and rigid; finally, the system was reheated to recover its original shape at the previous temperature, and the recovery time recorded when the recovery angle was 30°, 60°, 90°, 120°, 150° and 180°.

## RESULTS AND DISCUSSION

### Feasibility Analysis

In our experimental, we hope that the second-stage curing is not be triggered during the first curing stage. Therefore, we are validating the feasibility of two different curing stages. Non-isothermal DSC is utilized to investigate the curing process of various mixtures. The DSC curves are shown in Figure 3, and the peak temperatures and reaction heat enthalpies are listed in Table II.

From Figure 3(a), showing the DSC curve of E-51/593 mixture, it can be seen that the peak temperature is 94.4°C, then, in Figure 3(b), revealing the curing curve of E-51/594 system, the peak temperature is quite high (218.3°C). The difference between the peak temperatures of the E-51/593 and E-51/594 system is about 120°C. The relatively large temperature difference is favoring to two-step independent curing, as we anticipate. Figure 3(c) presents two mutual independent curing peaks, suggesting that a two-step curing process has been implemented successfully in the E-51/593/594 mixtures. However, the temperature of the second curing peak (182.6°C) in Figure 3(c) is lower than that in Figure 3(b). This can be explained by the fact that the test process of non-isothermal DSC is a continuous heating mode, which is different from the curing schedules (2)

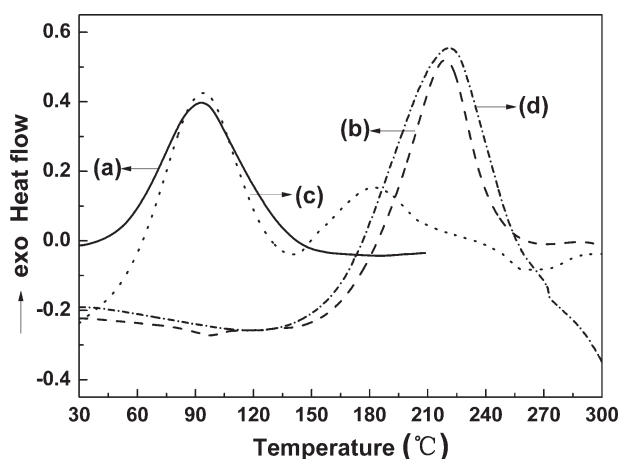


**Figure 3.** DSC curves of various mixtures in 10°C/min heating rate. (a) E-51/593; (b) E-51/594; (c) E-51/593/594 continuous heating; (d) E-51/593/594 cooling for 2 h.

**Table II.** Peak Temperatures and Reaction Heat Enthalpies of the DSC Curves

System	Peak temperature (°C)		Reaction heat enthalpy (J/g)	
	Peak one	Peak two	Peak one	Peak two
E-51/593	94.4	-	160.8	-
E-51/594	-	218.3	-	164.1
E-51/593/594 continuous heating	94.0	182.6	176.3	73.3
E-51/593/594 cooling for 2 h	-	221.6	-	170.6

and leads to a greater reaction heat in the mixtures. This reaction heat can not dissipate fast enough, so the second stage curing step has been triggered in advance, resulting in a lower peak temperature (182.6°C), as shows in Figure 3(c). The phenomenon has been also reflected in the reaction heat enthalpies. The reaction heat enthalpies of Figure 3(c)-peak two is lower than Figure 3(b) base on same proportion systems, indicating that the chemical reaction between latent curing agent and E-51 has been triggered during the non-isothermal DSC test.

In order to solve this problem, we modify the test method as follows: first, the E-51/593/594 system is tested by non-isothermal DSC in 10°C/min from 20 to 130°C. Second, we stop the test and allow the mixture to cool slowly until room temperature. Then it stays for 2 h at room temperature. Finally, the system is heated again from 20 to 380°C in 10°C/min heating rate. From Figure 3(d) the curve presents only a second stage curing peak, and there is no curing exothermic peak between 20°C and 150°C, indicating that first stage curing is complete. This peak temperature (221.6°C) of this second stage curing is near to the peak temperature (218.3°C) in Figure 3(b), and the reaction heat enthalpy (170.6 J/g) is similar to E-51/594 mixture (164.1 J/g) too. It manifests that the first curing stage hardly influences the second curing stage.

The DSC test results prove that the two different curing stages are implemented successfully, and the effect between the two step curing is rare, they can occur independently.

#### FTIR Analysis

FTIR spectra of various mixtures are shown in Figure 4. We use the FTIR test to detect the epoxy absorption peaks in different composites. Generally speaking, the characteristic absorption peak of epoxy group is 908~930 cm<sup>-1</sup>, so the wavenumber from 700 to 1000 cm<sup>-1</sup> has been magnified in Figure 4(b). In the EP70, EP80, EP90, EP70 I, EP80 I, and EP90 I systems, the characteristic absorption peaks of epoxy groups are observed in the range of 910~928 cm<sup>-1</sup>. Furthermore, the area of peaks reduces as the curing degree decreasing, illustrating that the epoxy groups reacts with curing agents appropriately. On the other hand, in the EP II mixtures, the characteristic absorption peaks of epoxy groups are hardly noticeable. It presents that remaining epoxy groups have reacted with the latent curing agent; in other words, the second curing has been triggered, and the reaction is complete.

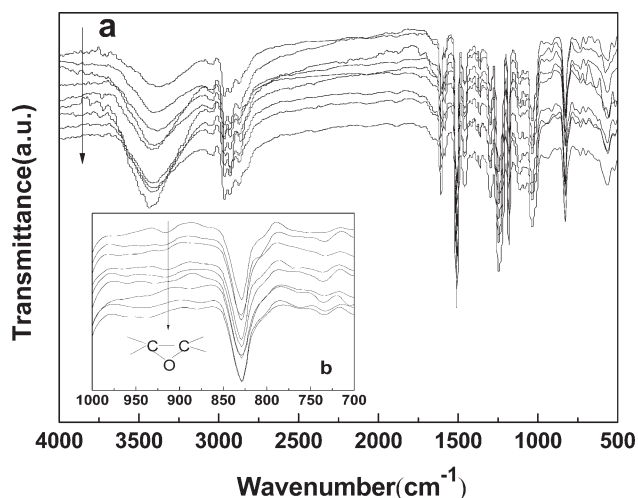


**Figure 4.** FTIR spectra of various mixtures. From above to below these are: EP70, EP80, EP90, EP70 I, EP80 I, EP90 I, EP70 II, EP80 II, and EP90 II.

The FTIR test results reveal that second curing can be achieved using cure schedule (2) successfully; in addition, the latent curing agent reacts completely with the remainder of the epoxy resin.

#### Shape-Memory Performance

In this research, we use EP70 and EP70 I systems as examples to discuss the shape memory effect of materials I by above fold-deploy shape-memory test method. Figure 5 shows the shape recovery ratio of EP70 and EP70 I mixtures at different temperatures. The results show that all mixtures can recover to their original shapes (180° return angle) within 1.5 min, so the shape recovery ratio is 100%. It suggests that the materials possess excellent shape-memory properties. Comparing Figure 5(a) and (b), the shape recovery time is similar under their respective  $T_g$ ,  $T_g + 10^\circ\text{C}$ ,  $T_g + 20^\circ\text{C}$ , and  $T_g + 30^\circ\text{C}$ , indicating that the addition of latent curing agent has little effect on the shape-memory recovery properties. Meanwhile, the shape recovery time reduces with increase of temperature. It can be explained as follows: when the temperature increases, the segments are given a greater free volume and larger room to move, allowing an increase in thermal motion of molecules and molecular chains; therefore, friction between the chains is reduced, and the samples do a faster recovery of their original shape. Furthermore, the recovery speed of 0–120° return angle is faster than 120–180° return angle. Because of the inner stress leading shape recovery releases fast at the beginning, and then releases slower gradually with inner stress reduction. Finally, the inner stress is almost running out, so the recovery speed is slow. The EP70 and EP70 I systems can be fold-deploy for ten times circulation without fracture.

For EP70 II, EP80 II and EP90 II mixtures, rigidity prevents them to bending into a “U” shape under 300°C, hence, we believe that the materials II have better stability, it cannot be deformed easily by external force though the temperature is high.

#### Tensile Strength Analysis

In this research, the tensile test has been done to discuss the mechanical properties of materials. Figure 6 shows the tensile

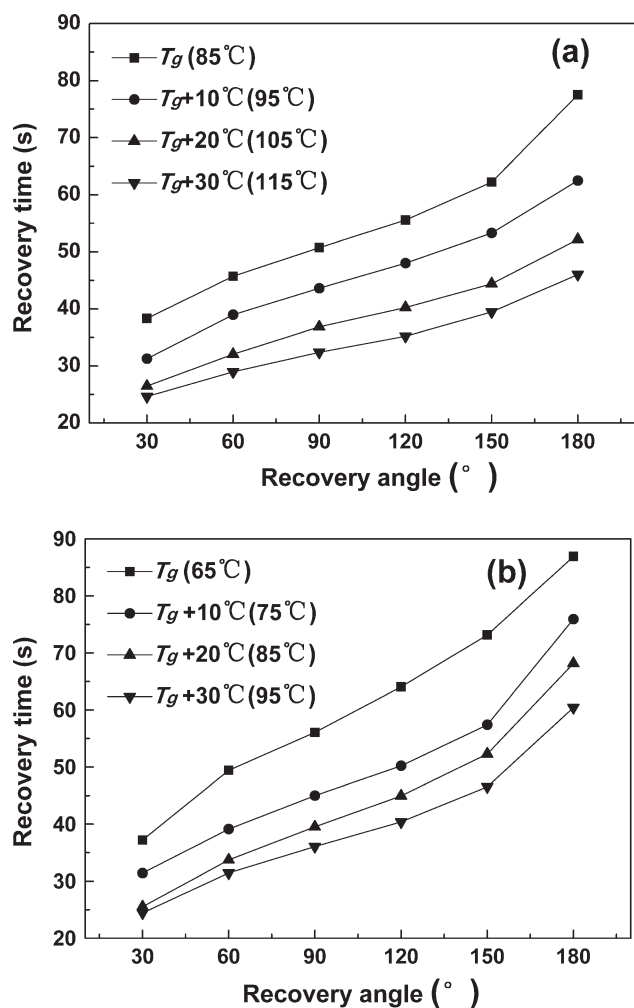


**Figure 5.** The effect of temperature on the shape recovery ratio: (a) EP70; (b) EP70 I.

strength of EP, EP I, and EP II mixtures at 60, 70, 80, and 90% theoretical curing degree, respectively. It can be seen that the tensile strength has been enhanced with the theoretical curing

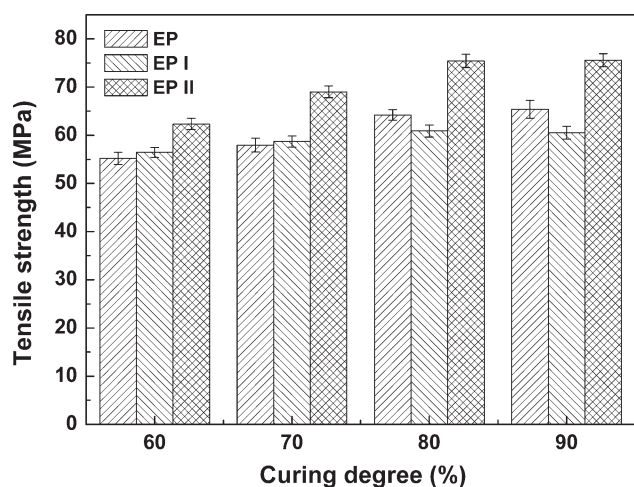


**Figure 6.** The tensile strength of EP, EP I, and EP II mixtures at 60, 70, 80, and 90% theoretical curing degree.

degree increase. Due to the higher theoretical curing degree have higher crosslink-density, more crosslink nets can be formed to resist external tensile. Moreover, compare with EP and EP I composites, the tensile strength of EP 60 I and EP70 I is same to EP 60 and EP70, meanwhile, EP 80 I and EP 90 I is lower than EP80 and EP90 systems. It can be explained as follows: the latent curing agent has bulky molecular structure [Figure 2(c)], in addition, it is not react with matrix resins during first stage curing, thus the molecule lead to steric hindrance influence. The steric hindrance effect reduces the crosslink density as well as decreases crosslink nets to resist external tensile. And that, the space steric effect with the increase of cure degree is more obvious. Furthermore, the tensile strength of EP II mixtures increases 12.9–19.0% compared with the EP system, suggesting that the tensile strength has improved significantly. Due to second curing stage has been triggered under schedule (2) condition, the unreacted epoxy groups have reacted with the latent curing agent to form more crosslink nets.

### SEM Analysis

SEM micrographs for various tensile fracture of composites are shown in Figure 7. Among all, the fracture surface of the neat matrix is smooth in Figure 7(a), suggesting a brittle rupture. With the addition of latent curing agent, the fracture surface becomes a little ragged and feather-like, which indicates that toughness has a little enhanced in Figure 7(b). This result is consistent with tensile strength analysis, the addition of latent curing agent reduces crosslink-density. Moreover, Figure 7(c–e) all shows striated fracture surfaces, illustrating that the fracture mechanism and surface structure of EP II are similar after second-stage curing. In other words, the curing reaction between the remainder epoxy resin and latent curing agent is completed, as proved by FTIR analysis.

The above analysis demonstrates that the addition of latent curing agent barely changes the fracture mechanism; all the fractured surfaces exhibits brittle rupture. Moreover, second-stage curing can be triggered to react completely.

### DMA Analysis

Figure 8 shows the glass transition temperature ( $T_g$ ) of different systems. From Figure 8(a), it can be seen that the  $T_g$  of EP70 II mixture is much higher than EP70 and EP70 I, as a result of the triggering of the second curing which leads to an increase in crosslink-density. It proves that the heat resistance of material has been enhanced effectively by the second curing stage. In addition,  $T_g$  of EP70 I mixture is lower than the EP70 system. This can be explained by the bulky molecular structure of the latent curing agent [Figure 2(c)] causing steric hindrance and reduced crosslink-density, when it mixes with matrix resin without reaction to any of the groups. It is consistent with tensile strength analysis. Generally speaking, crosslink-density is one of most important influencing factors for  $T_g$ . Hence, the lower crosslink-density would lead to a lower  $T_g$ . Furthermore, the peak height of  $\tan \delta$  curves can characterize the damping properties of materials. This can be explained as follows: with the increases of crosslink-density, more crosslink nets can be formed. These crosslink nets limit the free movement of many

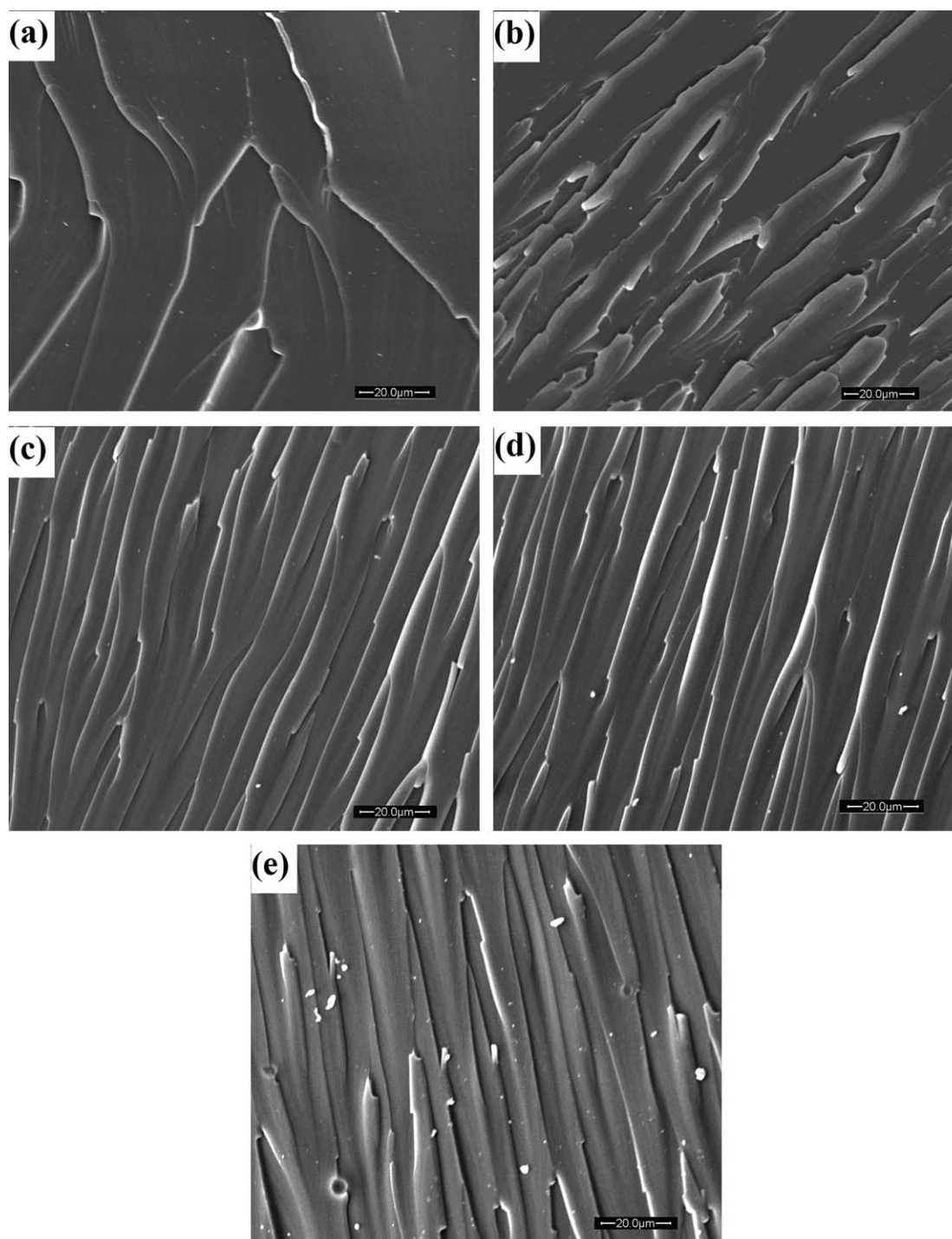


**Figure 7.** SEM micrographs of the fracture surface for varies mixtures. (a) EP70, (b) EP70 I, (c) EP70 II, (d) EP80 II, and (e) EP90 II.

chains, so the internal friction decreases as well as damping; hence, the reduction of peak height.

Figure 8(b) presents  $T_g$  in different curing degree mixtures which have resulted from second stage curing. Among the  $\tan \delta$  curves of EP II, it is noted that the broad peaks appeared in the left shoulder, suggesting that EP II may be occurred as a phase separation. It is consistent with the observed phenomenon in

experiments: the cured EP and EP I systems are translucent, and cured EP II mixtures are light yellow in color. However, the phase separation can not be observed in SEM micrographs, because the two phases are all cured epoxy curing groups that possess a similar color. On the other hand, the curves show that the  $T_g$  is near among EP II systems, suggesting that the curing degree has reached nearly 100%. It indicates that the latent

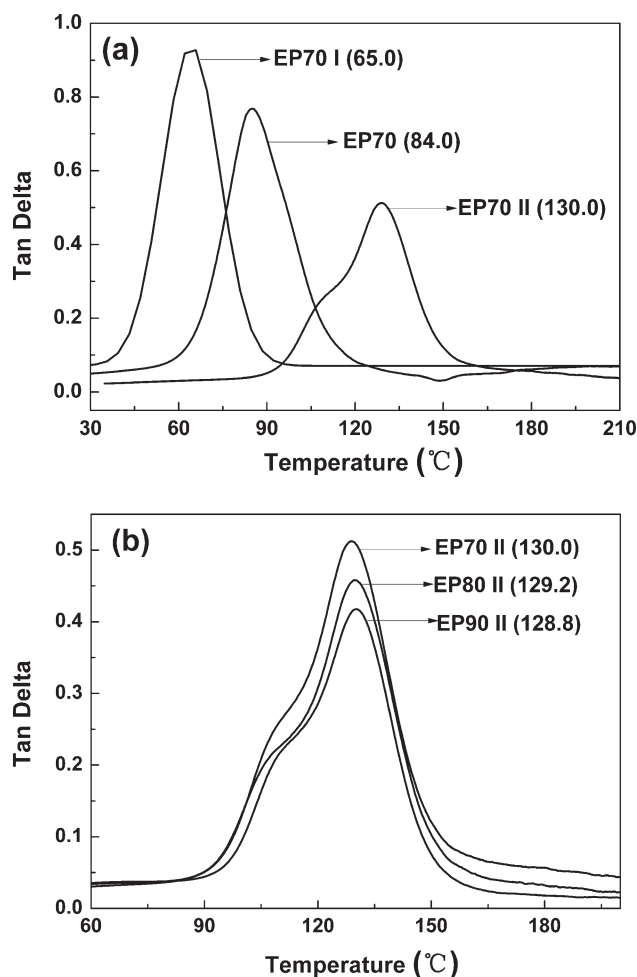


Figure 8. The DMA curves of various mixtures.

curing has been triggered successfully and the remaining uncured epoxy groups in the first curing stage react completely with latent curing agent. Here, the mixtures rarely contain active groups, such as epoxy groups, primary amine, secondary amine, and so on.

The DMA test results demonstrate that the second curing stage has been triggered successfully under cure schedule (2), while the curing reaction goes to completion; in addition, heat resistant properties has been improved, and  $T_g$  has been enhanced from 84.0 to 130.0°C.

## CONCLUSION

In this article, we used the new two-stage curing method to prepare a series of mixtures. The results of DSC tests showed that the two different curing stages could be implemented independently, and the interaction between the two different curing stage was little. Moreover, the fold-deploy shape-memory tests proved that EP70 and EP70 I possessed excellent shape-memory properties. They could be deformed into different shapes, then recover fully to their original shape within 1.5 min at  $T_g$ , the shape recovery ratio could reach 100%, and could be fold-

deploy for 10 times. The stability of EP II polymers had been reinforced by second stage curing due to they could not be deformed at 300°C. Tensile tests results suggested that the tensile strength had been enhanced about 12.9–19.0% after the second curing stage. SEM results revealed that the addition of latent curing agent did not change the fracture mechanism; all the surface fractures were brittle. Furthermore, DMA results presented that  $T_g$  had been boosted from 84.0 to 130.0°C, indicating that the heat resistance of materials had been improved significantly after second curing stage.

## REFERENCES

- Xie, T. *Polymer* **2011**, *52*, 4985.
- Huang, W. M.; Ding, Z.; Wang, C. C.; Wei, J.; Zhao, Y.; Purnawali, H. *Mater. Today* **2010**, *13*, 54.
- Harekrishna, D.; Niranjana, K. *J. Appl. Polym. Sci.* **2010**, *116*, 106.
- Behl, M.; Lendlein, A. *Mater. Today* **2007**, *10*, 20.
- Song, W. B.; Wang, Z. D. *J. Appl. Polym. Sci.* **2013**, *128*, 199.
- Lendlein, A.; Jiang, H. *Nature* **2005**, *434*, 879.
- Mohr, R.; Kratz, K. *Proc. Natl. Acad. Sci. USA* **2006**, *10*, 3540.
- Sun, L.; Huang, W. M.; Ding, Z. *Mater. Design* **2012**, *33*, 577.
- Tetwiler, D. A.; Lesser, A. J. *J. Mater. Sci.* **2012**, *47*, 3493.
- Liang, C.; Rogers, C. A.; Malafeev, E. *J. Int. Mater. Syst. Struct.* **1997**, *4*, 380.
- Psarras, G. C.; Parthenios, J.; Galiotis, C. *J. Mater. Sci.* **2001**, *36*, 535.
- Xie, T.; Rousseau, I. A. *Polymer* **2009**, *50*, 1852.
- Alteheld, A.; Feng, Y.; Kelch, S.; Lendlein, A. *Angew. Chem. Int. Ed.* **2005**, *44*, 1188.
- Feng, Y.; Behl, M.; Kelch, S.; Lendlein, A. *Macromol. Biosci.* **2009**, *9*, 45.
- Feng, Y.; Xue, Y.; Guo, J.; Lei, C. *J. Appl. Polym. Sci.* **2009**, *112*, 473.
- Paderni, K.; Pandini, S.; Passera, S.; Pilati, F.; Toselli, M. *J. Mater. Sci.* **2012**, *47*, 4354.
- Lendlein, A.; Kelch, S. *Angew. Chem. Int. Ed.* **2002**, *41*, 2034.
- Liu, C.; Qin, H.; Mather, P. T. *J. Mater. Chem.* **2007**, *17*, 1543.
- Jiang, W.; Ding, Y. *Microelectron. Eng.* **2008**, *85*, 458.
- El-ghayoury, A.; Hofmeier, H. *Macromolecules* **2003**, *36*, 3955.
- Bagis, Y. H.; Rueggeberg, F. A. *Dent. Mater.* **2000**, *16*, 244.
- Liu, Y. Y.; Sun, H.; Tan, H. F.; Du, X. W. *J. Appl. Polym. Sci.* **2013**, *127*, 3152.
- Liu, Y. Y.; Han, C. M.; Tan, H. F.; Du, X. W. *Polym. Adv. Technol.* **2010**, *22*, 2017.
- Ratna, D.; Karger-Kocsis, J. *Polymer* **2011**, *52*, 1063.